

Electrostatic interactions in dissipative particle dynamics using the Ewald sums

Minerva González-Melchor, Estela Mayoral, María Eugenia Velázquez, and José Alejandro

Citation: *The Journal of Chemical Physics* **125**, 224107 (2006); doi: 10.1063/1.2400223

View online: <http://dx.doi.org/10.1063/1.2400223>

View Table of Contents: <http://scitation.aip.org/content/aip/journal/jcp/125/22?ver=pdfcov>

Published by the [AIP Publishing](#)

Articles you may be interested in

[Effective electrostatic interactions in solutions of polyelectrolyte stars with rigid rodlike arms](#)

J. Chem. Phys. **123**, 244901 (2005); 10.1063/1.2138695

[Coarse-grained molecular-dynamics simulations of the self-assembly of pentablock copolymers into micelles](#)

J. Chem. Phys. **123**, 234905 (2005); 10.1063/1.2137714

[Titration of hydrophobic polyelectrolytes using Monte Carlo simulations](#)

J. Chem. Phys. **122**, 094911 (2005); 10.1063/1.1856923

[Effects of solvent quality on the dynamics of polymer solutions simulated by dissipative particle dynamics](#)

J. Rheol. **46**, 1221 (2002); 10.1122/1.1498285

[The effect of acid-base equilibria on the fractional charge and conformational properties of polyelectrolyte solutions](#)

J. Chem. Phys. **114**, 2830 (2001); 10.1063/1.1334677



Re-register for Table of Content Alerts

Create a profile.



Sign up today!



Electrostatic interactions in dissipative particle dynamics using the Ewald sums

Minerva González-Melchor^{a)}

Instituto de Física, Universidad Autónoma de Puebla, Apartado Postal J-48, 72570 Puebla, Mexico

Estela Mayoral and María Eugenia Velázquez

Centro de Investigación en Polímeros, grupo COMEX, Marcos Achar Lobatón No. 2, Tepexpan, 55885 Acolman, Estado de México, Mexico

José Alejandro^{b)}

Departamento de Química, Universidad Autónoma Metropolitana-Iztapalapa, Avenida San Rafael Atlixco 186, Colonia Vicentina, 09340 México DF, Mexico

(Received 7 August 2006; accepted 27 October 2006; published online 14 December 2006)

The electrostatic interactions in dissipative particle dynamics (DPD) simulations are calculated using the standard Ewald [Ann. Phys. **64**, 253 (1921)] sum method. Charge distributions on DPD particles are included to prevent artificial ionic pair formation. This proposal is an alternative method to that introduced recently by Groot [J. Chem. Phys. **118**, 11265 (2003)] where the electrostatic field was solved locally on a lattice. The Ewald method is applied to study a bulk electrolyte and polyelectrolyte-surfactant solutions. The structure of the fluid is analyzed through the radial distribution function between charged particles. The results are in good agreement with those reported by Groot for the same systems. We also calculated the radius of gyration of a polyelectrolyte in salt solution as a function of solution pH and degree of ionization of the chain. The radius of gyration increases with the net charge of the polymer in agreement with the trend found in static light scattering experiments of polystyrene sulfonate solutions. © 2006 American Institute of Physics. [DOI: [10.1063/1.2400223](https://doi.org/10.1063/1.2400223)]

I. INTRODUCTION

The dissipative particle dynamics (DPD) simulation method¹ was developed to accomplish the task of reaching larger lengths and longer time scales than atomistic molecular dynamics (MD) simulations, resulting in a mesoscopic description of the system.^{2,3} This approach has been successfully applied to study a wide variety of complex fluids including polymeric solutions, colloidal suspensions, surfactants, and biological membranes,^{4,5} where different lengths and time scales are involved. The DPD method was originally proposed to study repulsive soft interactions but it has been modified to include multibody effects^{6,7} which allow the inclusion of attractive interactions to simulate vapor-liquid equilibrium.⁸ We have recently shown that finite size effects in DPD simulations⁹ are less important than in microscopic simulations, hence it is possible to simulate systems using a small number of particles.

For all the complex systems mentioned above, the electrostatic interactions play a key role in understanding phenomena that do not occur in noncharged systems. So the inclusion of these interactions in DPD simulations is essential to capture phenomena at mesoscopic level such as formation of polyelectrolyte-surfactant aggregates, charge stabilization of colloidal suspensions, and the formation of complexes driven by charged species in biological systems.

Electrostatic interactions were recently included in DPD by Groot.¹⁰ He proposed a method where the electrostatic field is solved locally on a grid. The method was applied to study an electrolyte and a polyelectrolyte-surfactant solution among other systems. He stated that the method was reasonably efficient, can treat local inhomogeneities in dielectric permittivity, and it captures the most important features of electrostatic interactions.

On the other hand, the Ewald sum method¹¹ is the most employed route to calculate electrostatic interactions in microscopic molecular simulations. It is widely accepted that it is the best technique to treat Coulombic forces and extensive effort has been done to improve its efficiency.¹²⁻¹⁴ The Ewald sum method can also be used in combination with techniques to include polarization, see Refs. 15 and 16 and references therein. The main problem in using the Ewald method in DPD simulations is that electrostatic interactions between DPD particles are soft and atoms with opposite charge form artificial clusters of ions. The main goal of this work is to show that the standard Ewald sum method combined with charge distributions on particles to avoid the formation of nondesirable ionic pairs can be used to calculate the electrostatic interactions in mesoscopic simulations. The method proposed in this work is easily implemented in standard DPD programs. The inclusion of charge distributions does not increase the computational cost in the Ewald sum procedure. However, the method might be computationally more demanding than that used by Groot.¹⁰ The efficiency can be improved by using techniques that allow fast calcula-

^{a)}Electronic mail: minerva@sirio.ifuap.buap.mx

^{b)}Electronic mail: jra@xanum.uam.mx

tion of the reciprocal part such as the smooth particle mesh Ewald.¹² By using charge distributions on DPD particles it is possible to use a polarization version of the Ewald sums to simulate systems having regions with different dielectric constants. The proposed method was applied to study a bulk electrolyte and an aqueous solution of polyelectrolyte-surfactant mixture. These systems were studied by Groot and we make the corresponding comparison to validate our results. In addition, the method was applied to calculate structural properties of a polyelectrolyte in a salt solution as a function of the net charge fraction on the polymer and solution pH.

The rest of this work is organized as follows: Section II contains the description of the DPD method. Our proposal to treat electrostatic interactions is presented in Sec. III. The comparison with Groot's results on structural properties of ionic systems is contained in Sec. IV. Section V gives the end-to-end distance and radius of gyration of a polyelectrolyte in solutions with salt added as a function of the charge fraction on the polymer and as a function of solution pH. Finally, main conclusions are given.

II. THE DPD APPROACH

The DPD method was introduced by Hoogerbrugge and Koelman.¹ The main conceptual difference with atomistic dynamics is the coarse-graining procedure that allows the mapping of several molecules from the real system into one DPD particle. In this section we give a general description of the method; more details are found in Ref. 3. In DPD simulations a set of interacting particles is considered and the total force, \mathbf{F}_{ij} , between any pair of particles i and j is the sum of a conservative \mathbf{F}_{ij}^C , a dissipative \mathbf{F}_{ij}^D , and a random \mathbf{F}_{ij}^R force,

$$\mathbf{F}_{ij} = \mathbf{F}_{ij}^C + \mathbf{F}_{ij}^D + \mathbf{F}_{ij}^R. \quad (1)$$

These forces are given by

$$\mathbf{F}_{ij}^C = a_{ij} \omega^C(r) \hat{\mathbf{e}}_{ij},$$

$$\mathbf{F}_{ij}^D = \gamma \omega^D(r) [\hat{\mathbf{e}}_{ij} \cdot \mathbf{v}_{ij}] \hat{\mathbf{e}}_{ij},$$

$$\mathbf{F}_{ij}^R = \sigma \omega^R(r) \hat{\mathbf{e}}_{ij} \xi_{ij}, \quad (2)$$

where $\hat{\mathbf{e}}_{ij} = \mathbf{r}_{ij}/r$, $\mathbf{r}_{ij} = \mathbf{r}_i - \mathbf{r}_j$, $\mathbf{v}_{ij} = \mathbf{v}_i - \mathbf{v}_j$, r is the distance between particles i and j and \mathbf{r}_i and \mathbf{v}_i are the position and velocity of particle i , respectively. The random force is calculated using a random number ξ_{ij} which is uniformly distributed between 0 and 1 with Gaussian distribution, zero mean, and unit variance. The constants a_{ij} , γ , and σ determine the strength of the conservative, dissipative, and random forces, respectively. The weight functions ω 's are given by

$$\omega^C(r) = \omega^R(r) = \sqrt{\omega^D(r)} = \omega(r), \quad (3)$$

with

$$\omega(r) = \begin{cases} 1 - r/R_c, & r \leq R_c \\ 0, & r > R_c, \end{cases} \quad (4)$$

being R_c the cutoff distance. The intramolecular interaction in the polyelectrolyte and surfactant molecules, which have more than one particle in their structure, is given by harmonic forces, so that if atoms i and j are bonded,

$$\mathbf{F}_{ij}^B = -K(r - r_0) \mathbf{r}_{ij}/r, \quad (5)$$

where K is the spring constant and r_0 is the equilibrium bond distance.

The dissipative and random forces are related through the fluctuation-dissipation theorem ($\sigma^2 = 2\gamma k_B T$), generating naturally the canonical distribution (constant number of particles, N , volume, V , and temperature, T). The forces \mathbf{F}_{ij}^D and \mathbf{F}_{ij}^R act as an in-built thermostat. Here k_B is the Boltzmann's constant. In this standard DPD formulation the conservative forces consist of a short-range repulsive interaction modeling the soft nature of neutral DPD particles. Electrostatic interactions are conservative long-range forces that must be taken into account to capture electrostatic phenomena. Once Coulombic interactions are included, the total conservative forces will determine the thermodynamic behavior of the system. The next section describes our proposal to calculate electrostatic interactions in DPD.

III. THE EWALD SUMS AND CHARGE DISTRIBUTIONS

The method proposed in this work consists of a combination of charge distributions on DPD particles and the Ewald sum technique, widely used to calculate electrostatic forces.

A set of N DPD particles, every one carrying a point charge q_i at positions \mathbf{r}_i in a cubic cell of side L and volume $V = L^3$, is considered. Overall charge neutrality is assumed. Charges interact according to Coulomb's law, and the total electrostatic energy for the periodic system is given by

$$U(\mathbf{r}^N) = \frac{1}{4\pi\epsilon_0\epsilon_r} \sum_i \sum_{j>i} \sum_{\mathbf{n}} \frac{q_i q_j}{|\mathbf{r}_{ij} + \mathbf{n}L|}, \quad (6)$$

where $\mathbf{n} = (n_x, n_y, n_z)$, n_x, n_y, n_z are integer numbers and the prime means that terms with $i=j$ are omitted when $\mathbf{n}=0$. The variables ϵ_0 and ϵ_r are dielectric constants of vacuum and water at room temperature, respectively. The sum over \mathbf{n} takes into account the periodic images. In the Ewald treatment the long-range electrostatic energy, Eq. (6), is decomposed in a real space and the reciprocal space contributions.^{11,17} In this way, the real and the reciprocal parts are both short-ranged sums written as

$$U(\mathbf{r}^N) = \frac{1}{4\pi\epsilon_0\epsilon_r} \left[\sum_i \sum_{j>i} q_i q_j \frac{\text{erfc}(ar)}{r} + \frac{2\pi}{V} \sum_{\mathbf{k} \neq 0} Q(\mathbf{k}) S(\mathbf{k}) S(-\mathbf{k}) - \frac{\alpha}{\sqrt{\pi}} \sum_i^N q_i^2 \right], \quad (7)$$

with

$$Q(k) = \frac{e^{-k^2/4\alpha^2}}{k^2}, \quad S(\mathbf{k}) = \sum_{i=1}^N q_i e^{i\mathbf{k}\cdot\mathbf{r}_i}, \quad \mathbf{k} = \frac{2\pi}{L}(m_x, m_y, m_z), \quad (8)$$

where α is the parameter that controls the contribution in the real space, k is the magnitude of the reciprocal vector \mathbf{k} , whereas m_x , m_y , and m_z are integer numbers. Equation (7) is a good approach to $1/r$ given by Eq. (6), capturing the full long-range nature of electrostatic interactions. The electrostatic interactions between two DPD particles are calculated whether the particles are bonded or not.

In DPD methodology, the conservative force appearing in Eq. (2) is mathematically well defined at $r=0$, allowing full overlap between particles. However, the electrostatic contribution diverges at $r=0$, leading to the formation of artificial ionic pairs. To avoid this problem, Groot¹⁰ used a charge distribution given by

$$\rho(r) = \frac{3}{\pi R_e^3}(1 - r/R_e), \quad (9)$$

for $r < R_e$, where R_e is a smearing radius. For $r > R_e$, $\rho(r) = 0$. To calculate the electrostatic forces, Groot followed the method of Beckers *et al.*,¹⁸ where the electrostatic field is solved on a lattice. The charge distributions were spread out over the lattice nodes and the long-range part of the interaction potential was calculated by solving the Poisson equation in real space. It was stated that the method works efficiently if the grid size is equal to the particle size. As the grid size is reduced there is an improvement on the accuracy of the electrostatic forces but the CPU time increases.

In this work, in order to remove the divergency at $r=0$ we consider a charge distribution on DPD particles of the form

$$\rho(r) = \frac{q}{\pi\lambda^3}e^{-2r/\lambda}, \quad (10)$$

where λ is the decay length of the charge. This function is a Slater-type charge density appearing in the context of quantum mechanical calculations. When Eq. (10) is integrated over the space the total charge is q .

The functional form of the charge density might be completely arbitrary but the forces cannot in general be calculated analytically; however, for a distribution given by Eq. (10), good approximated expressions for the force are available.^{19,20} In what follows, reduced units are employed to compare with Groot's results. To make the length, energy, and mass dimensionless, we used R_c , $k_B T$, and particle mass, respectively. In what follows $R_c^* = (k_B T)^* = m^* = 1$. The reduced interaction potential between two charged distributions separated by a distance r^* from center to center is given by¹⁹

$$\frac{4\pi u^*(r^*)}{\Gamma} = \frac{Z_i Z_j}{r^*} [1 - (1 + \beta^* r^*) e^{-2\beta^* r^*}], \quad (11)$$

where Z_i is the valence of ion i , e is the electron charge, $\Gamma = e^2/(k_B T \epsilon_0 \epsilon R_c)$, and $\beta^* = R_c/\lambda$. The value R_c is obtained from $R_c = (\rho^* N_m V_m / N_A)^{1/3}$ where ρ^* is the reduced density of DPD particles, N_m is the number of real water molecules

inside a DPD particle, $V_m = 18 \text{ cm}^3 \text{ mol}^{-1}$ is the molar volume of water, and N_A is Avogadro's number. Therefore, $R_c = 4.48 N_m^{1/3} \text{ \AA}$ and $\Gamma = 20.08 N_m^{-1/3}$. Groot used $N_m = 3$, hence $R_c = 6.46 \text{ \AA}$ and $\Gamma = 13.87$. Taking $N_m = 3$ and $a_{ii} = 78.33$ between solvent particles, the compressibility of pure water at room temperature is reproduced.²¹ In systems with salt, the molar concentration of salt was calculated¹⁰ using $c^{\text{real}} = (N_{\text{NaCl}}/V^*)/(R_c^3 N_A)$ where N_{NaCl} is the number of salt molecules.

The magnitude of the reduced force between two charge distributions is

$$\frac{4\pi F_{ij}^{*e}}{\Gamma} = \frac{Z_i Z_j}{r^{*2}} \{1 - e^{-2\beta^* r^*} [1 + 2\beta^* r^* (1 + \beta^* r^*)]\}. \quad (12)$$

Equations (11) and (12) contain the Coulombic term which can be calculated in a simulation using the standard Ewald scheme. By including the charge distribution, the divergency of the Coulomb interactions at $r^* = 0$ was removed. In the limit $r^* \rightarrow 0$, the energy and the force between two charged distributions are finite quantities, they are given by

$$\lim_{r^* \rightarrow 0} \frac{4\pi u^*(r)}{\Gamma} = Z_i Z_j \beta^* \quad (13)$$

and

$$\lim_{r^* \rightarrow 0} \frac{4\pi F_{ij}^{*e}}{\Gamma} = 0, \quad (14)$$

respectively. In this work β^* was chosen to match the interaction between two charge clouds at $r^* = 0$ proposed by Groot,¹⁰ whose expression reduces in this limit to

$$\lim_{r^* \rightarrow 0} \frac{4\pi u^{*\text{Groot}}(r^*)}{\Gamma} = \frac{52}{35} \frac{Z_i Z_j}{R_e^*}. \quad (15)$$

Comparing Eqs. (13) and (15) we obtain

$$\beta^* = \frac{52}{35 R_e^*} \approx 0.929. \quad (16)$$

Once β^* is obtained the potential energy and forces are calculated using Eqs. (11) and (12), respectively. The Coulombic term is then evaluated using the Ewald sums. Figure 1 shows the interaction between charged particles with the same sign as calculated in this work. The electrostatic interactions used by Groot¹⁰ were slightly different and they were calculated from a lattice method in a real space. The theoretical curve corresponding to the charge distributions studied by Groot are also shown in Fig. 1. The maximum value of the force in both models is about the same, but the force used in this work is shifted to smaller distances making the repulsive interactions larger than in Groot's model. An opposite behavior is observed for the attractive forces.

The total conservative force is thus given by adding \mathbf{F}_{ij}^{*e} from Eq. (12) to \mathbf{F}_{ij}^C in Eqs. (2). These forces will determine the thermodynamic behavior of the system.

According to Ruelle's test²² a system has a well defined thermodynamic behavior if the total interaction energy satisfies two requirements: first, the interaction between distant particles must be negligible and second, it must satisfy the

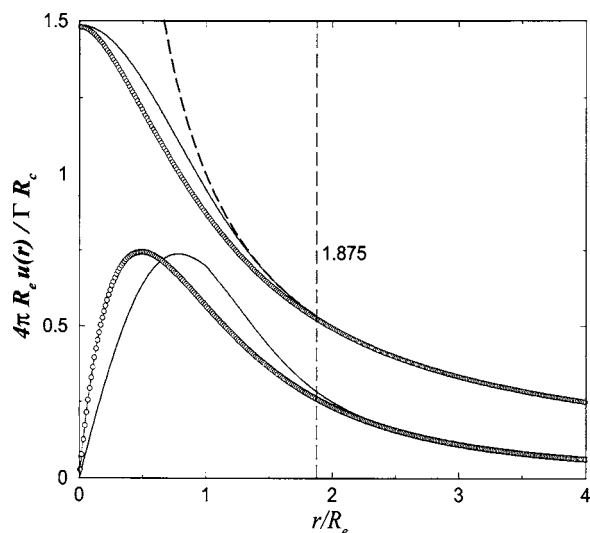


FIG. 1. Electrostatic potential (upper curves) and force (lower curves) between two equal-sign charge distributions. The theoretical electrostatic interaction and the force used by Groot (Ref. 10) are shown with continuous lines. The open circles represent the electrostatic interaction and the force employed in this work, given by Eqs. (11) and (12). The vertical dashed line is the distance $R_c^{\text{real}}/R_c = 1.875$ at which the real part was truncated. R_c^{real} was taken equal to $R_c^{\text{real}} = 3.0R_c$ and $R_e = 1.6R_c$. The dashed line is the Coulombic $1/r$ potential, which diverges at $r=0$.

so-called stability definition.²² The latter establishes the fact that the interaction must not cause the collapse of an infinite number of particles into a bounded region. If a given potential does not satisfy this condition it is called a catastrophic potential. Different interactions have been analyzed in terms of its stability such as the Gaussian core model²³ and the electrostatic interaction between charge distributions. This latter was analyzed by Fisher and Ruelle.²⁴ They concluded that a system with charge density on particles, rather than point charges, is stable. Furthermore, as stated in Refs. 22 and 24, if a positive pair interaction potential is added to a stable one, the total interaction in the system remains stable. Here it follows that the total potential energy used in this work should give the right thermodynamic behavior.

IV. COMPARISON WITH GROOT'S RESULTS

To validate the method of calculating the electrostatic interactions proposed in this work, a comparison with Groot's results was made for two systems: (A) bulk electrolyte and (B) aqueous solution of polyelectrolyte-surfactant mixture. The DPD particles were moved using the modified version of the velocity Verlet algorithm, DPD-VV.²⁵

A. Bulk electrolyte

As a first case of study, we present the simple electrolyte studied by Groot.¹⁰ We used his same set of parameters to make a direct comparison with his results. Electrostatic interactions were calculated following the method described in Sec. III. The system consists of a total number of $N=3000$ DPD particles in a simulation cell of volume $V^*=10 \times 10 \times 10$. The solvent mimicking water at room temperature has 2804 DPD particles while 98 particles represent ions with net charge e and the same number, carrying a net charge of $-e$,

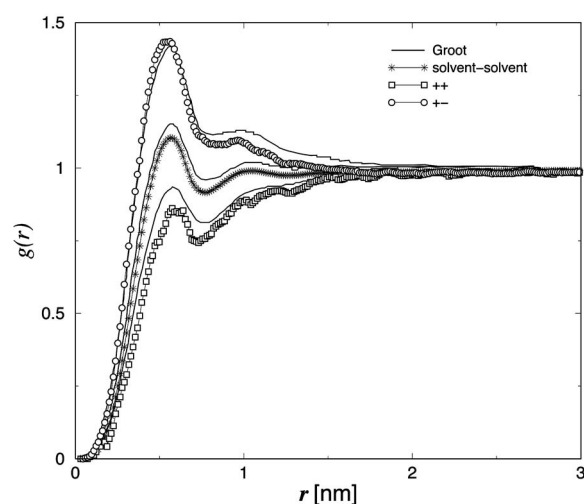


FIG. 2. Comparison between RDFs obtained by Groot (Ref. 10) and the method proposed here. The repulsive parameters were set to $a_{ij}=25.0$ and $R_c=6.46$ Å.

represent the counterions. The total number density is $\rho^*=3.0$. Mapping these quantities to real units, the system corresponds to a salt concentration of $0.6M$. The interaction parameters for the conservative, dissipative, and random forces were $a_{ij}=25.0$, $\lambda=4.5$, and $\sigma=3.0$, respectively. The same value of a_{ij} was used for the interaction between any two DPD particles. We note that $a_{ij}=25.0$ corresponds to $N_m=1$ instead of $N_m=3$, but that was the value that Groot used in his work.

A reduced time step of $\Delta t^* = \Delta t(k_B T / m R_c^2)^{1/2} = 0.02$ was used during the simulation. The real forces in the Ewald sums were truncated at $R_c^{\text{real}} = 3.0R_c$ with $\alpha = 0.15$ Å⁻¹. For the reciprocal part we considered the sum with a maximum vector $\mathbf{k}^{\text{max}} = (5, 5, 5)$. The value of $\beta^* = 0.929$, obtained in Eq. (16), was used in all simulations. The average temperature in all simulations is the same as the imposed external value.

The structure of solvent and ions was determined by the radial distribution functions (RDFs). The results from this work and those obtained by Groot¹⁰ are shown in Fig. 2. A general good agreement is observed. The first point to look at is that there is no ionic formation at distances close to $r=0$. The structure between ions carrying the same charge is slightly lower than those obtained by Groot because the interaction model used in this work is more repulsive at short distances. One would expect that the maximum in the RDF of the particles with opposite charge moved to shorter distances and had a higher value respect to Groot's results. However, the RDF is almost the same at short distances, this means that DPD repulsive interactions compensate the attraction of ions with opposite charge. It is seen that water is slightly less structured than in Groot's work.

In Ref. 10 the reduced quantities to calculate the electrostatic interactions were obtained using $N_m=3$ but he used the repulsion parameter $a_{ij}=25$ which corresponds to $N_m=1$. Those values, $a_{ij}=25$ and $N_m=3$, do not change the conclusions drawn in his work. The radial distribution functions obtained for the bulk electrolyte using $a_{ij}=78.3$ ($N_m=3$) are

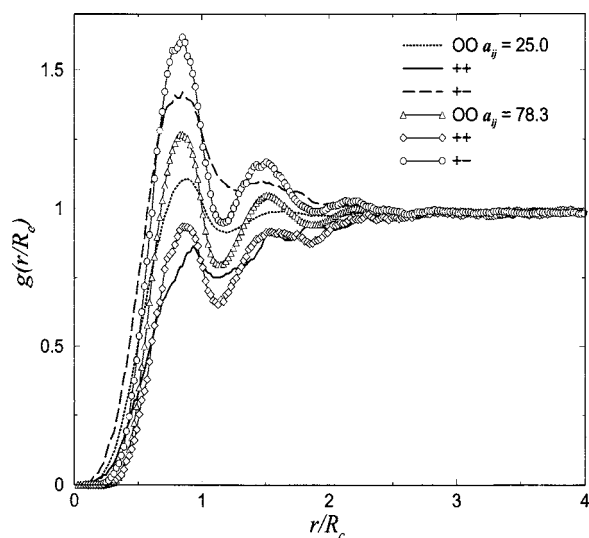


FIG. 3. Comparison between RDFs for two different values of the repulsion parameter: $a_{ij}=25.0$, shown with dotted, continuous and dashed lines; and $a_{ij}=78.33$ shown with the symbols displayed on the figure.

shown in Fig. 3 and they are compared with results from $a_{ij}=25$. The position of the first maximum is around the same value for both coarse graining levels. Although the density is the same, the fluid is more structured when $N_m=3$ because the interaction between particles is more repulsive.

B. Aqueous solution of polyelectrolyte-surfactant mixture

The system consists of a total number of $N=10\,125$ DPD particles. The polymer (50 monomers) corresponds to a molecular weight $M_w=8000$; water (9825 particles) and surfactant molecules (75 particles) were allocated in a cubic box of volume $V^*=15 \times 15 \times 15$. The interaction parameters were the same as those used by Groot. Each monomer on the polymer carries a net charge of $e/2$. Anionic surfactant molecules were modeled as head-tail dimers. The head groups carry a net charge $-e$ and tails are represented by neutral particles. To preserve charge neutrality in the system 25 polymer counterions of charge $-e$ and 75 surfactant ions of net charge e were added. A harmonic force between bonded particles in the polyelectrolyte and surfactant molecules was used. The spring constant was $K=4.0$ and the bond equilibrium distance was zero. The repulsive interaction parameters a_{ij} for the cross interactions in a system with $\rho^*=3$ were obtained¹⁰ through

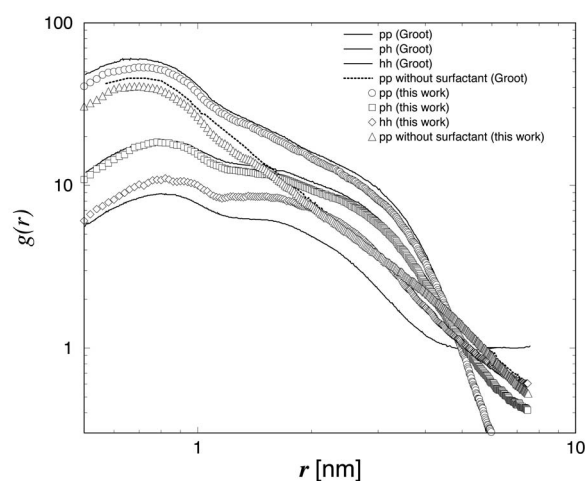


FIG. 4. Comparison between RDFs obtained by Groot (Ref. 10) and the method proposed here. The system consists of a polyelectrolyte in solution, surfactant molecules, and the corresponding counterions (system B). The symbols are read as follows: intramolecular polymer-polymer (circles), polymer-head group (squares), and head group-head group (diamonds). The intramolecular polymer-polymer RDF for the system with surfactant replaced by salt is shown with triangles. For comparison, the data obtained by Groot (Ref. 10) for the same systems are plotted with solid (polyelectrolyte-surfactant-solvent) and dotted lines (polyelectrolyte-salt-solvent).

$$a_{ij} = a_{ii} + \chi_{ij}/0.306, \quad (17)$$

where χ_{ij} is the Flory-Huggins interaction parameter. The parameters a_{ij} are given in Table I for completeness. The time step used was $\Delta t^*=0.04$ and after equilibration the average properties were obtained from 2×10^5 time steps of production time. It is convenient to mention again that $a_{ii}=25$ for the solvent used by Groot corresponds to $N_m=1$.

Figure 4 shows selected RDFs for a polyelectrolyte in the presence of surfactant molecules. The agreement between results from this work and those from Ref. 10 is excellent for polymer-polymer (pp) and polymer-head (ph) interactions. The RDF from this work for the head-head (hh) particles is systematically lower than those reported by Groot due to higher repulsion between those particles at short distances. The effect is magnified at large distances. In this work the electrostatic interactions do not include polarization effects in contrast with the results reported in Ref. 10 where water and head groups carried out large polarizabilities. That is another difference in our model that might explain the differences found for the head-head RDF. The RDF for polyelectrolyte particles without surfactant is also in excellent agreement with Groot's data. The slopes on RDF between $1 \text{ nm} < r < 2.8 \text{ nm}$ obtained in this work for the polymer-

TABLE I. Repulsive interaction parameters between DPD particles for the polyelectrolyte-surfactant system.

a_{ij}	Solvent	Tail	Head	Monomer	Surfactant ion	Counterion
Solvent	25.0	83.8	25.0	27.1	25.0	25.0
Tail	83.8	25.0	44.6	44.6	25.0	25.0
Head	25.0	44.6	25.0	25.0	25.0	25.0
Monomer	27.1	44.6	25.0	25.0	25.0	25.0
Surfactant ion	25.0	25.0	25.0	25.0	25.0	25.0
Counterion	25.0	25.0	25.0	25.0	25.0	25.0

polymer pairs were -1.3 and -1.9 for systems with and without surfactant, respectively. These values compared well with those reported by Groot, -1.18 and -1.90 , respectively.

V. RESULTS OF POLYELECTROLYTE IN SOLUTION WITH SALT ADDED

The main results of this section are the end-to-end distance, $\langle R_{ee}^2 \rangle^{1/2}$, and the radius of gyration, $\langle R_g^2 \rangle^{1/2}$, of a polyelectrolyte in solution as a function of dissociation degree. The radius of gyration is a property that has been widely studied, both experimentally^{26,27} and theoretically,^{28,29} to correlate changes in polymer conformation with different physicochemical and biological properties. It is known that in a polyelectrolyte, $\langle R_g^2 \rangle^{1/2}$ depends on the solution pH because the net charge on the polymer changes with it. $\langle R_g^2 \rangle^{1/2}$ is also dependent on counterion concentration, for this reason most of studies are carried out with a fixed amount of salt added or constant ionic strength.

A. End-to-end distance and radius of gyration

In this section we present DPD simulation results of a single polyelectrolyte in water as function of the polymer charge in the presence of salt. Five charge fractions, defined by $\theta = N_q/N_p$, were considered. Here N_q is the number of charged beads on the chain and N_p is the total number of beads conforming the polymer. Going from a neutral to a fully ionized polymer, θ takes the values 0, 0.24, 0.48, 0.76, and 1.0, containing $N_q=0, 12, 24, 38$, and 50 charged beads, respectively. The charge distributions of magnitude $e/2$ were assigned uniformly to different beads on the chain. Counterions of charge density $-e$ were added to preserve charge neutrality. All systems contained 75 salt molecules which give 75 cations (net charge e) and 75 anions (net charge $-e$). The total number of beads in the system was $N=10\,125$ in all cases.

Each simulation involved $N_p=50$ polymer beads in a simulation cell of volume $V^*=15 \times 15 \times 15$ in the presence of solvent, salt, and counterions. The solution corresponds to a salt concentration of $0.14M$. The total density was fixed at $\rho^*=3$. The equilibrium bond distance r_0 was set to zero and the spring constant was $K=4.0$.

The repulsive interaction between beads was obtained through $a_{ij}=a_{ii}+\chi_{ij}/0.306$, where $a_{ii}=78.3$. The parameter χ_{ij} for polymer and water was $\chi_{pw}=0.65$, taken from Ref. 10. In this way, for polymer and water $a_{pw}=80.42$ and $a_{ij}=78.3$ for the other species.

TABLE II. Reduced end-to-end distance and radius of gyration as function of the fraction of charge θ going from a neutral to a fully ionized polymer.

θ	$\langle R_{ee}^2 \rangle^{1/2}$	$\langle R_g^2 \rangle^{1/2}$
0.00	6.5 ± 1.0	2.9 ± 0.2
0.24	7.2 ± 0.7	3.1 ± 0.2
0.48	8.3 ± 1.0	3.5 ± 0.2
0.76	9.6 ± 1.7	3.9 ± 0.4
1.00	10.9 ± 1.7	4.4 ± 0.4

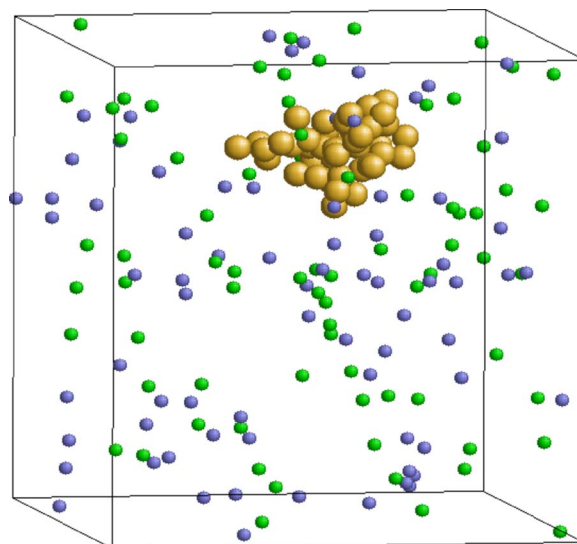


FIG. 5. Typical conformation of a neutral polyelectrolyte in a salt solution of $0.14M$.

Conformational properties of the polyelectrolyte as a function of the fraction charge θ are summarized in Table II. The end-to-end distance and $\langle R_g^2 \rangle^{1/2}$ for this linear chain increase monotonically with the degree of ionization. Experimentally it is well known²⁹ that a neutral polymer in solution with salt has the smallest radius of gyration compared either with a partially or a fully ionized chain. Figures 5 and 6 show instantaneous snapshots of a neutral and a fully ionized polyelectrolyte in solution with salt. It is seen that ionization elongates the chain in agreement with experimental findings. The value of $\langle R_{ee}^2 \rangle^{1/2}$ and $\langle R_g^2 \rangle^{1/2}$ for the fully ionized chain is 1.7 and 1.5 times larger than that found for the neutral polymer, respectively. These results are evidence that the method used in this work for calculating the electrostatic forces gives the right trend on $\langle R_g^2 \rangle^{1/2}$ for a charged polymer.

For a 1:1 electrolyte at room temperature the Debye

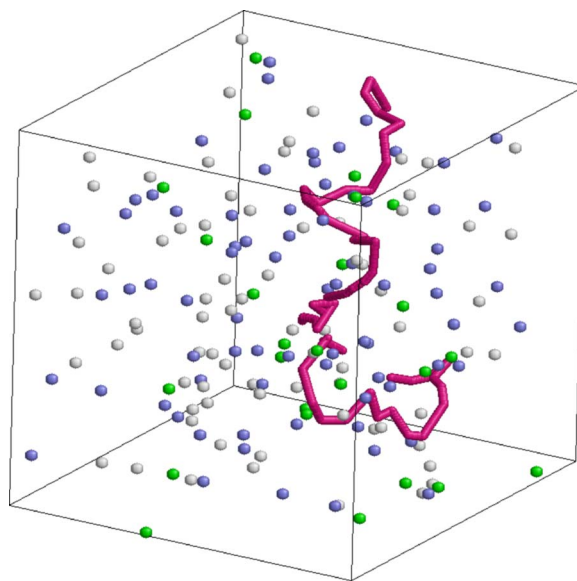


FIG. 6. Typical conformation of a fully ionized polyelectrolyte in a salt solution of $0.14M$.

screening length is given by $l_D = 3.045C^{-1/2} \text{ \AA}$, where C is the molar concentration. For systems simulated in Secs. IV A and V A, the Debye screening lengths are 3.9 and 8.1 \AA , respectively. At these concentrations the Debye-Hückel theory predicts that the interactions between charged particles separated further than 3.9 and 8.1 \AA become screened and the interaction is no longer long range. However, the Debye-Hückel theory is valid for very diluted electrolytes and is not expected to be valid for highly concentrated systems. A more recent generalized Debye-Hückel theory has been developed where the screening length has become spatially dependent, in this way a local effect of the charges^{30,31} is introduced. The method presented here has the advantage that any salt concentration can be studied. The system studied in Sec. IV A was chosen for comparison purposes while that in Sec. V A was chosen as a simple polymer model at a moderate concentration. It is very likely that a smaller cut-off radius for the real forces could have been used but details concerning this sort of optimization were not studied in this work, nevertheless they are necessary to justify the choice of parameter values used in the Ewald method.

An important issue is the range of concentrations where explicit salt ions can be replaced by a screened interaction potential between particles. This topic is beyond the scope of the present work. It deserves special attention and certainly is a study that will be undertaken.

Concerning the decay of correlations in systems with electrostatic interactions, some simulation works and several theoretical calculations have been done in terms of the parameter x defined by $x = \kappa a$, where κ is the inverse Debye screening length $\kappa = 1/l_D$ and a is the diameter of the particle.^{32,33} For a certain value of x , called the Kirkwood parameter, x_K , the behavior of the structural correlation function crosses from a simple screened monotonic decay for $x < x_K$, to an oscillatory decay for $x > x_K$. We have not analyzed the decay behavior of correlations in the DPD fluids presented here. Focus on this issue requires a more detailed analysis and is left for future work.

B. Effect of solution pH on radius of gyration

In addition, we studied the behavior of the radius of gyration of a weak monoprotic polyacid as a function of pH and fraction of net charge θ (the number of charged monomers divided by the total amount of ionizable monomers) on

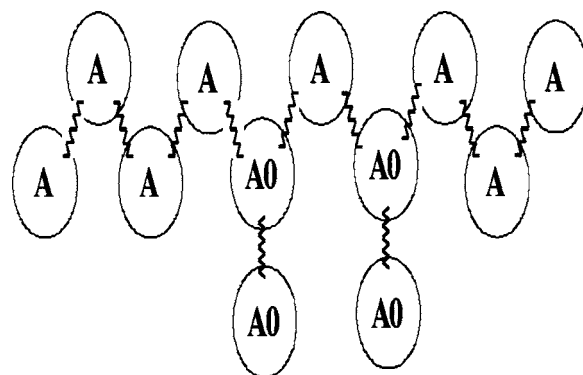


FIG. 7. Scheme of the polyelectrolyte used in this work, A can take the forms A^- (ionized) and $A0$ (neutral).

the polymer, at a constant amount of salt. Experimentally, the net charge of the polyelectrolyte can be fixed by changing the system's pH. We can relate the pH with the fraction of net charge by

$$pH = \log_{10} \left(\frac{\theta}{1 - \theta} \right) + pK_a, \quad (18)$$

where pK_a is the acidity constant; in this work pK_a was chosen to be 5.5 which is a typical value of a weak polyelectrolyte. This equation was obtained considering that initially the polymer is fully deprotonated. As H^+ ions are added, the polyelectrolyte starts to protonate reaching an equilibrium where there is a balance of dissociated species.

In our model the polyelectrolyte is a branched chain that contains two different groups, one of this is neutral and the other one is a monoprotic acid. This molecule can be mapped into 12 DPD beads, as shown in Fig. 7. As the pH is modified, the four $A0$ beads remain neutral while the other eight (A in Fig. 7) can be $A = A0$ or $A = A^-$ if they are ionized according to Eq. (18). So for a given value of pH we fix a charge distribution of net charge $-e$ on the DPD polymer beads which are randomly chosen and that charge remains fixed during the simulation.

We consider that each DPD particle contains three real water molecules, $N_m = 3$. The reduced density was $\rho^* = 3$ in a cubic box of reduced box length of 8.5. The repulsive interaction parameters³⁴ between two particles were $a_{ij} = 78.33$ except for $A0$ -water, $A0$ - Cl^+ , and $A0$ - A^- where $a_{ij} = 79.33$, respectively. The number of particles of each species used in

TABLE III. Number of particles used in simulations, $A^- = A$ ionized, $A0 = A$ neutral, $I^+ =$ polymer counterion. The salt concentration is 0.01M, a typical experimental value.

θ	pH	Na^+	Cl^-	I^+	A^-	$A0$	H_2O
0.0	1.00	1	1	0	0	12	1816
0.125	4.62	1	1	1	1	11	1816
0.25	4.99	1	1	2	2	10	1816
0.375	5.25	1	1	3	3	9	1816
0.5	5.47	1	1	4	4	8	1816
0.625	5.69	1	1	5	5	7	1816
0.75	5.95	1	1	6	6	6	1816
0.875	6.32	1	1	7	7	5	1816
1.0	14.00	1	1	8	8	4	1816

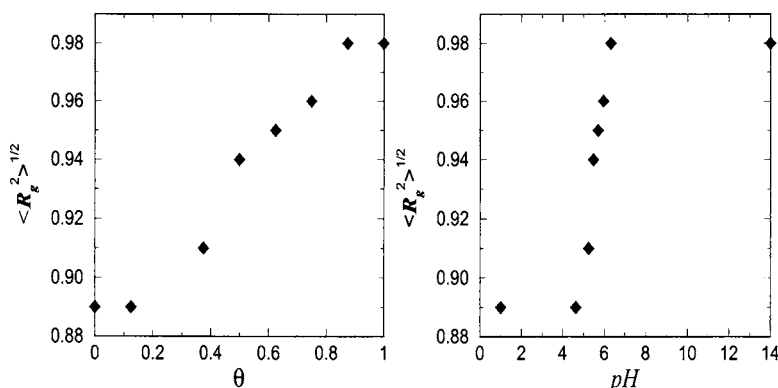


FIG. 8. $\langle R_g^2 \rangle^{1/2}$ as a function of net charge fraction on the polymer (left side) and as a function of pH (right side).

our simulations, is listed in Table III. After equilibration, the averages were obtained over 350 000 time steps. When beads are bonded the equilibrium bond distance r_0 was zero and the spring constant was $K=100$. The reduced time step was $\Delta t^*=0.04$.

Figure 8 on the left-hand side shows results for $\langle R_g^2 \rangle^{1/2}$ as a function of θ from simulations of this work. The trend agrees with the experimental results for a weak polyelectrolyte.²⁹ On the right-hand side of Fig. 8 are also shown the results obtained for radius of gyration as a function of pH. We can see an inflexion point around the pH value of the polyelectrolyte's pK_a , which agrees qualitatively with observed experimental results.²⁶ It is important to point out that the pH values of 1 and 14 correspond to the fully protonated and fully ionized polyelectrolyte structures, respectively.

VI. CONCLUSIONS

An alternative method to Groot's¹⁰ implementation to treat electrostatic interactions in DPD simulations is proposed. Charge distributions are assigned to charged DPD particles to avoid the formation of artificial ion pairs. The long-range term $1/r$ is calculated via the standard Ewald sum scheme. The proposed method makes use of conservative interactions with a well defined stable thermodynamic behavior and it is easily implemented in DPD simulation programs. It can also be combined with fast Fourier transform techniques to improve the calculation of the reciprocal space part. Electrostatic interactions with different dielectric constants might be calculated using the Ewald sum method combined with techniques to include polarization. The method proposed in this work was compared with the results obtained by Groot and good agreement was found for the radial distribution functions of charged particles in a bulk electrolyte solution and in a polyelectrolyte-surfactant mixture. When it was applied to study polyelectrolytes in solution the obtained electrostatic forces give the right experimental trend on radius of gyration as a function of polymer ionization and as a function of solution pH as that found in experiments.

ACKNOWLEDGMENTS

This work was supported by Centro de Investigación en Polímeros, Grupo COMEX. One of the authors (M.G.M.)

thanks R. D. Groot for helpful correspondence on this topic. The authors also thank T. A. Darden and A. Gama for useful discussions.

- ¹ P. J. Hoogerbrugge and J. M. V. A. Koelman, *Europhys. Lett.* **19**, 155 (1992).
- ² P. Español and P. B. Warren, *Europhys. Lett.* **30**, 191 (1995).
- ³ R. D. Groot and P. B. Warren, *J. Chem. Phys.* **107**, 4423 (1997).
- ⁴ R. D. Groot, *Langmuir* **16**, 7493 (2003).
- ⁵ T. Murtola, E. Falck, M. Patra, M. Karttunen, and I. Vattulainen, *J. Chem. Phys.* **121**, 9156 (2004).
- ⁶ S. Y. Trofimov, E. L. F. Nies, and M. A. J. Michels, *J. Chem. Phys.* **117**, 9383 (2002).
- ⁷ I. Pagonabarraga and D. Frenkel, *J. Chem. Phys.* **115**, 5015 (2001).
- ⁸ P. B. Warren, *Phys. Rev. E* **68**, 066702 (2003).
- ⁹ M. E. Velázquez, A. Gama-Goicochea, M. González-Melchor, M. Neria, and J. Alejandre, *J. Chem. Phys.* **124**, 084104 (2006).
- ¹⁰ R. D. Groot, *J. Chem. Phys.* **118**, 11265 (2003).
- ¹¹ P. P. Ewald, *Ann. Phys.* **64**, 253 (1921).
- ¹² U. Essmann, L. Perera, M. L. Berkowitz, T. Darden, H. Lee, and L. G. Pedersen, *J. Chem. Phys.* **103**, 8577 (1995).
- ¹³ M. Deserno and C. Holm, *J. Chem. Phys.* **109**, 7678 (1998).
- ¹⁴ C. Sagui and T. Darden, *J. Chem. Phys.* **114**, 6578 (2001).
- ¹⁵ C. Haibo Yu, T. Hansson, and W. F. van Gunsteren, *J. Chem. Phys.* **118**, 221 (2003).
- ¹⁶ A. Toukmaji, C. Sagui, J. Board, and T. Darden, *J. Chem. Phys.* **113**, 10913 (2000).
- ¹⁷ D. Frenkel and B. Smit, *Understanding Molecular Simulations, From Algorithms to Applications* (Academic, New York, 1996).
- ¹⁸ J. V. L. Beckers, C. P. Lowe, and S. W. de Leeuw, *Mol. Simul.* **20**, 369 (1998).
- ¹⁹ M. Carrillo-Tripp, Ph.D. thesis, *Universidad Autónoma del Estado de Morelos*, 2005.
- ²⁰ H. Saint-Martin, J. Hernández-Cobos, M. I. Bernal-Uruchurtu, I. Ortega-Blake, and H. J. Berendsen, *J. Chem. Phys.* **113**, 10899 (2000).
- ²¹ B. Hafskjold, C. Liew, and W. Shinoda, *Mol. Simul.* **30**, 879 (2004).
- ²² D. Ruelle, *Statistical Mechanics: Rigorous Results* (World Scientific, Singapore/Imperial College Press, London, 1999).
- ²³ A. A. Louis, P. G. Bolhuis, and J. P. Hansen, *Phys. Rev. E* **62**, 7961 (2000).
- ²⁴ M. E. Fisher and D. Ruelle, *J. Math. Phys.* **7**, 260 (1966).
- ²⁵ I. Vattulainen, M. Karttunen, G. Besold, and J. M. Polson, *J. Chem. Phys.* **116**, 3967 (2002).
- ²⁶ P. C. Griffiths, A. Paul, Z. Khayat, K.-W. Wan, S. M. King, I. Grillo, R. Schweins, P. Ferruti, J. Franchini, and R. Duncan, *Biomacromolecules* **5**, 1422 (2004).
- ²⁷ E. Nordmeier, *Polym. J.* **25**, 1 (1993).
- ²⁸ D. Stigter and K. A. Dill, *Macromolecules* **28**, 5325 (1995).
- ²⁹ D. Stigter and K. A. Dill, *Macromolecules* **28**, 5338 (1995).
- ³⁰ B. P. Lee and M. E. Fisher, *Phys. Rev. Lett.* **76**, 2906 (1996).
- ³¹ H. Frusawa, R. Hayakawa, *Phys. Rev. E* **61**, R6079 (2000).
- ³² R. J. F. Leote de Carvalho, R. Evans, and Y. Rosenfeld, *Phys. Rev. E* **59**, 1435 (1999).
- ³³ B. P. Lee and M. E. Fisher, *Europhys. Lett.* **39**, 611 (1997).
- ³⁴ R. D. Groot and K. L. Rabone, *Biophys. J.* **81**, 725 (2001).